

# Normalized Shear Modulus of Compacted Gravel

## Module de cisaillement normalisé des graviers compactés

Liao T., Massoudi N., McHood M.  
Bechtel Power Corporation, Frederick, MD, USA

Stokoe K.H., Jung M.J., Menq F.-Y.  
University of Texas, Austin, TX, USA

**ABSTRACT:** Compacted gravel is often used as engineered fill to provide the needed bearing capacity for structures. The dynamic properties of the gravel fill, such as nonlinear shear modulus, are required in seismic analyses to evaluate the response to dynamic loading. From a series of Resonant Column and Torsional Shear (RCTS) tests on two types of crushed gravel fill, normalized shear modulus reduction curves were obtained as a function of cyclic shear strain. These curves are presented and compared to empirical relationships in the literature that have been proposed for gravelly soils.

**RÉSUMÉ:** Le gravier compacté est souvent utilisé comme remplissage pour fournir la capacité portante nécessaire aux structures. Les propriétés dynamiques du remblai de gravier, tels que le module non linéaire de cisaillement, sont requises dans les analyses sismiques pour évaluer la réponse à un chargement dynamique. A partir d'une série d'essais à la colonne de résonance et d'essais de cisaillement en torsion sur deux types de gravier concassé de remplissage, les courbes d'évolution du module de cisaillement normalisé ont été obtenues en fonction de la contrainte de cisaillement cyclique. Ces courbes sont présentées et comparées à des relations empiriques provenant de la littérature qui ont été proposées pour les sols graveleux.

**KEYWORDS:** Shear Modulus, Resonant Column Test, Torsional Shear Test, Fill, Gravel.

## 1 INTRODUCTION

Compacted gravel is frequently used as engineered fill beneath the foundations of important structures, such as nuclear power facilities and high-rise buildings. To evaluate the seismic response of the ground supporting these structures, the dynamic properties of the gravel fill (i.e., shear modulus  $G$  and material damping ratio  $D$ ) need to be determined. Due to the limited paper length, only normalized shear modulus is discussed herein.

Although the small-strain shear modulus ( $G_{\max}$ ) can be determined under in-situ conditions from shear wave velocity ( $V_s$ ) measured in the field, it is very difficult to obtain strain-dependent curves of  $G$  and  $D$  directly from in-situ tests (Ishihara 1996). In current engineering practice, the effects of confining pressure ( $\sigma_0$ ) and shear strain ( $\gamma$ ) on  $G$  and  $D$  are primarily evaluated through laboratory tests, such as cyclic triaxial (CTX), cyclic simple shear (CSS), cyclic torsional shear (TS), and resonant-column (RC) tests. These tests not only give the values of  $G$  and  $D$  at small strain, but also yield the variation of  $G$  and  $D$  with  $\gamma$  and  $\sigma_0$ . However, such tests are rarely performed on gravels, due to the large size of the testing apparatus required to test representative specimens. Additionally, because it is difficult to obtain undisturbed samples of gravelly soils, such tests on natural gravelly soil deposits have been mainly limited to high-quality undisturbed gravel samples obtained by in-situ ground freezing (e.g., Goto et al. 1992, 1994; Hatanaka and Uchida 1994; Kokusho and Tanaka 1994). Comparison of test results between undisturbed and reconstituted specimens show that the effect of sample disturbance is significant on  $G$ , but most researchers believe that it is quite small on  $G/G_{\max} \sim \gamma$  curves (e.g., Hatanaka and Uchida 1994; Rollins et al. 1998), although Kokusho and Tanaka (1994) indicate that undisturbed specimens exhibit greater degradation at relatively small strain levels.

## 2 LITERATURE REVIEW

By removing (or scalping) particles of size greater than 51 mm in diameter, Seed et al. (1986) performed a series of cyclic triaxial tests on 305-mm diameter specimens of four different types of well-graded gravels, which were isotropically-consolidated and tested under undrained cyclic loading conditions. Based on the test results, the  $G/G_{\max} \sim \log(\gamma)$  curves of gravelly soils are suggested to be in the range shown in Figure 1.

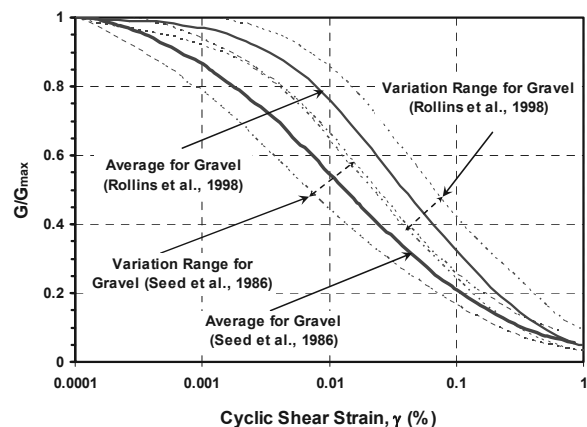


Figure 1. Typical  $G/G_{\max} \sim \gamma$  relationships for gravels.

By analyzing the test results for gravelly soils mainly found in literature, Rollins et al. (1998) also suggested a slightly different range for the  $G/G_{\max} \sim \log(\gamma)$  curves for gravelly soils (Figure 1). Most of the data used by Rollins et al. (1998) came from cyclic triaxial tests (CTS) typically performed on specimen of 300 mm in diameter and 600 mm in height, and a small portion of the tests are cyclic torsional simple shear tests performed on specimens of larger diameters. All these tests

were carried out at loading frequency in the range from about 0.01 Hz to 0.2 Hz.

Menq (2003) used both an RCTS device and an MMD (Multi-Mode Resonant) device to investigate the dynamic properties of gravelly soils. The RCTS device is capable of performing on the same soil specimen both the torsional resonant column (RC) test at high loading frequency (i.e., the resonant frequency) and in the nonlinear range and the cyclic torsional shear (TS) test at much lower frequencies, simply by changing the amplitude and frequency of the current in the drive coils and the motion monitoring devices used to record the specimen response (Isenhower 1979; Ni 1987; Hwang 1997). Because the same specimen can be subjected to both the RC and TS tests, it eliminates the variability due to testing different specimens or testing the same specimen subjected to a different stress history (Darendeli 2001). The test specimen for RC or TS testing typically has a diameter in range from 36 to 76 mm and a height from 72 to 152 mm (Menq and Stokoe 2003). To accommodate gravelly specimens with relatively large particle sizes, the MMD was developed and is capable of testing specimen with 152 mm in diameter and 600 mm in height in different measurement modes, including the torsional resonance mode similar to resonant column tests.

Based on the test results, Menq (2003) used the modified hyperbolic model suggested by Darendeli (2001) to model for shear modulus reduction of gravelly soils:

$$G/G_{\max} = 1/[1 + (\gamma/\gamma_r)^a] \quad (1)$$

$$\gamma_r = 0.12 \cdot C_u^{-0.6} (\sigma'_0/p_a)^{0.5C_u^{-0.5}} \quad (2)$$

$$a = 0.86 + 0.1 \cdot \log(\sigma'_0/p_a) \quad (3)$$

where the reference strain  $\gamma_r$  (%) is  $\gamma$  at  $G/G_{\max} = 0.5$ ,  $a$  is the curvature coefficient,  $C_u$  is the uniformity coefficient,  $\sigma'_0$  is the effective isotropic confining pressure, and  $p_a$  is the atmospheric pressure (1 atm).

### 3 MECHANICAL PROPERTIES OF TESTED GRAVEL

Two types of gravel were tested for potential use as engineered fill in this study. They are aggregates derived from processing crushed stone mined from a rock quarry, consisting of angular and hard particles, with one of them being poorly graded and designated as PA and the other being relatively well graded and designated as WA. Three batches of the WA material (WA-1, WA-2, and WA-3) and one batch of the PA material (PA-1) were taken for testing.

Modified Proctor tests in accordance with ASTM D1557 were performed on the WA material (WA-1 and WA-3) after removing/scalping particles greater than 19 mm in diameter. The modified Proctor test is not applicable to the PA material according to ASTM 1157. To be consistent with the modified Proctor test, all the other laboratory tests were also performed on the scalped material. Figure 2 shows the typical grain size distribution curves for the tested materials (i.e., PA and WA), as well as the grain size distribution curves of each batch of the material after scalping particles greater than 19 mm in diameter (i.e., PA-1, WA-1, WA-2, and WA-3).

In addition, maximum and minimum index densities were obtained based on ASTM 4254 and ASTM 4253 for both the PA material (PA-1) and the WA material (WA-1 and WA-3). As seen in Table 1, the maximum index density of the WA material determined using a vibratory table is very close to the maximum density obtained by impact compaction in which the moisture-density relationship is defined. But comparison shows that the maximum index density of the WA material is significantly (about 40%) higher than that of the PA material, which is understandable as the voids between the larger

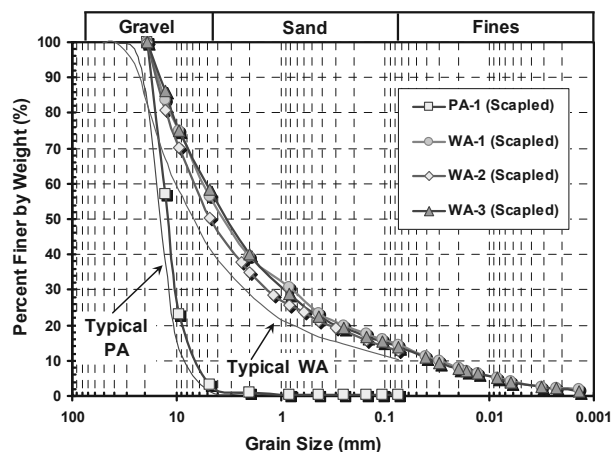


Figure 2. Grain size distribution curves of the unscalped and scalped (tested) gravel specimens.

particles of the WA material are filled with smaller particles.

From each batch of the material, a pair of specimens designated as A and B were created for the RCTS tests. The pair of specimens from each batch of the WA material were separately remolded at the optimum moisture content to approximately 95% and 100% of the maximum dry density determined in the modified Proctor test. And the pair of specimens of the PA material were remolded to relative densities of about 80% and 100% at a moisture content of about 1%. All specimens were compacted to the target densities using a hammer drill fitted with a specifically designed circular steel face of 146 mm in diameter.

After the RCTS tests were completed, more index tests such as the water content and dry density were performed on each specimen, and the results are summarized in Table 2, including the derived degrees of saturation and void ratio.

Table 1. Mechanical properties of scalped gravel samples.

Sample Name	Grain Size Distribution			$G_s$	Index Density ( $Mg/m^3$ )		Index Void Ratio		Moisture-Density Relationship	
	$D_{50}$ (mm)	$C_u$	$C_c$		$\rho_{\min}$	$\rho_{\max}$	$e_{\min}$	$e_{\max}$	$\rho_{\max}$ ( $Mg/m^3$ )	$w_{opt}$ (%)
PA-1	11.8	2.1	1.3	2.83	1.39	1.64	0.73	1.04	-	-
WA-1	3.4	174.5	3.81	2.72	1.67	2.30	0.18	0.62	2.31	0.653
WA-2	-	-	-	2.72	-	-	-	-	2.30	0.469
WA-3	3.2	150.6	4.87	2.82	1.67	2.27	0.24	0.69	2.34	0.653

Note:  $D_{50}$  is the particle diameter corresponding to 50% passing;  $C_c$  is the coefficient of curvature,  $G_s$  is the specific gravity, and  $w_{opt}$  is the optimum moisture content.

Table 2. Mechanical properties of gravel specimens tested in the RCTS device.

Sample Name	Specimen	Water Content (%)	Saturation (%)	Dry Density ( $Mg/m^3$ )	Void Ratio
PA-1	A	1	3.5	1.57	0.81
	B	0.8	3.2	1.66	0.70
WA-1	A	6.4	72.1	2.19	0.24
	B	6.1	85.5	2.27	0.19
WA-2	A	5.5	59.8	2.17	0.25
	B	4.4	65.3	2.30	0.18
WA-3	A	5.8	61.5	2.23	0.27
	B	6.2	87.2	2.35	0.20

### 4 RCTS TESTS ON COMPACTED GRAVEL

During RCTS testing, the specimen is sealed in a membrane, and the pore pressure in the specimen is vented to atmosphere pressure. From the results of cyclic triaxial tests on Toyoura sand, Kokusho (1980) indicated that the drained tests and the undrained tests give almost identical strain-dependent variation of the modulus within the strain level from 10<sup>-4</sup>% to 0.5%. Since the gravel specimens have larger permeability due to the

larger grain sizes and the maximum shear strain reached in the RCTS tests were less than 0.5%, the effect of the drainage condition was not expected to be significant on the measured dynamic properties.

For each gravel specimen, RCTS testing was performed at five effective isotropic confining pressures ( $\sigma_0'$ ) (i.e., 52, 207, 414, and 827 kPa). At each  $\sigma_0'$ , the specimen was first subjected to “consolidation” period up to 100 minutes. After 100 minutes, the TS tests and/or the RC tests were performed. If the TS test was performed, it was performed before the RC test, because the maximum strain amplitude reached in the TS test is generally lower than that in the RC test, leading to less potential disturbance in specimen.

During the TS test, hysteresis loops were generated from the measured torque and displacement at the top of the specimen. The slope of the line connecting the end points of the hysteresis loop is the secant shear modulus,  $G$ , representing the average shear stiffness of the soil at the peak strain in the test. Only TS test results at a loading frequency of 0.5 Hz and measured for the 10th cycle are presented here, as it best represents typical seismic loading (Zhang et al. 2005).

From the RC tests, a frequency response curve was obtained that shows the accelerometer output versus excitation frequency. The  $V_s$  is derived from the resonant frequency, with consideration of the specimen geometry and equipment characteristics. The shear modulus is then calculated using  $G = \rho V_s^2$ , where  $\rho$  is the mass density of the material.

For both the RC and TS tests, the variation of  $G$  as a function of increasing  $\gamma$  is determined by increasing the driving force in steps. The resulting  $G/G_{\max} \sim \log(\gamma)$  curves can be derived, taking as  $G_{\max}$  the  $G$  value measured at the lowest strain level (about  $10^{-4}\%$ ).

For the two PA specimens (i.e., PA-1-A and PA-1-B), the membranes around the specimens were punctured by the test material when the confining pressure was increased to 414 kPa, and thus no further test was carried out.

## 5 NORMALIZED SHEAR MODULUS OF COMPACTED GRAVEL

In Figures 3, the measured  $G/G_{\max} \sim \log(\gamma)$  curves for the specimens under the different confining pressures are presented. The circular and triangular symbols represent the measured data points from RC and TS tests, respectively, and the thin lines and thick lines connect data points of the WA specimens and PA specimens, respectively. The value of  $G/G_{\max}$  decreases with the increasing  $\gamma$  above a threshold strain ( $\gamma_t$ ) for all gravel specimens. This behavior is consistent with the observation of most researchers, except for Lin et al. (2000) who noticed that when shear strain surpassed 0.1%, the measured shear moduli of specimens with 60% and 80% of gravel content increase with increasing shear strain, and indicated this different behavior might be attributed to the effect of gap-graded grain size distribution. The values of  $\gamma_t$  range from about 0.00015% to 0.0005% for the WA specimens, and are slightly larger for the PA material, showing an increase as  $\sigma_0'$  increases, similar to Menq (2003)'s observation.

As noted above, the PA gravels behave more linearly than the WA material, which is consistent with Menq (2003)'s conclusion that the value of  $G/G_{\max}$  decreases as  $C_u$  increases. This difference is sometimes attributed to gravel content as observed by Rollins et al. (1998). It is interesting to note that for either gravel type (i.e., PA or WA), no consistent difference was found by grouping them by test type (RC or TS), which confirms that the  $G/G_{\max} \sim \log(\gamma)$  curves are not sensitive to loading frequency (Darendeli, 2001). The density (95% and 100% compaction for the WA samples, and 80% and 100% relative density for the PA samples) was not found to have a

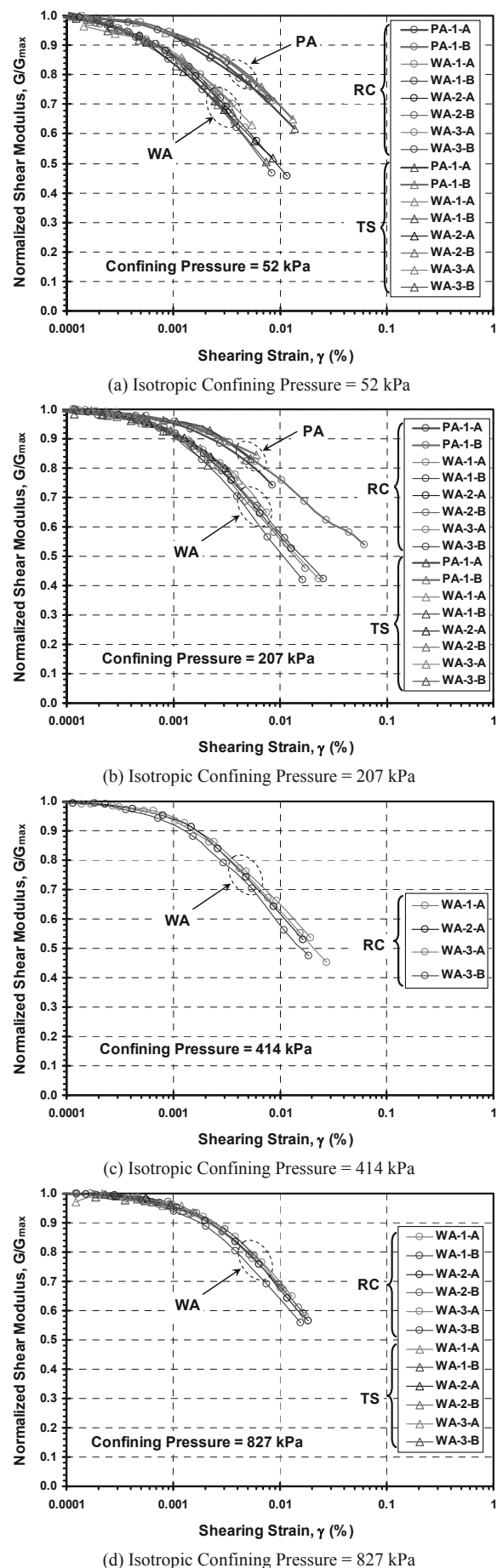


Figure 3.  $G/G_{\max} \sim \gamma$  curves for the specimens subject to RCTS tests.

significant effect on the  $G/G_{max} \sim \log(\gamma)$  curves, which agrees with Ishihara (1996)'s observation on sandy soils that the manner of shear modulus decreasing with strain is almost the same irrespective of the void ratio.

Figure 4(a) shows the average  $G/G_{max} \sim \log(\gamma)$  curves for the PA samples and the WA samples at different confining pressures, along with typical ranges for  $G/G_{max} \sim \log(\gamma)$  curves recommended by Seed et al. (1986) and Rollins et al. (1998). Similar to sandy material, the gravelly materials behave more linearly with increasing isotropic confining pressure. The comparison also shows that the curves for the WA samples generally fall in the ranges suggested by Seed et al. (1986), while those for the PA samples are more consistent with the  $G/G_{max} \sim \gamma$  range suggested by Rollins et al. (1998).

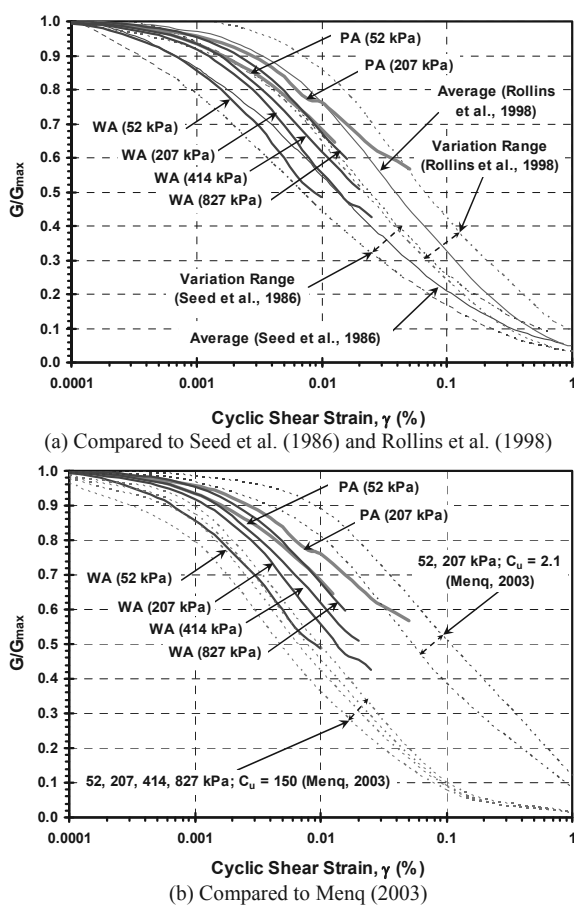


Figure 4.  $G/G_{max} \sim \log(\gamma)$  curves for compacted gravel in this study compared with gravel curves in the literature.

As shown in Table 1, the  $C_u$  values for WA-1 and WA-3 are 174.5 and 150.6, respectively, while it is 2.1 for PA. Taking  $C_u = 150$  and  $C_u = 2.1$  separately, the relationship between  $G/G_{max}$  and  $\gamma$  under different confining pressures can be predicted using the hyperbolic model proposed by Menq (2003) (i.e. Eq. (1)). Menq (2003)'s predictions are compared with the results from this study in Figure 4(b). The measured  $G/G_{max} \sim \log(\gamma)$  curves of the WA material degrade somewhat less than those predicted using Menq (2003), while the  $G/G_{max} \sim \log(\gamma)$  curves of the PA material degrade somewhat more than the predicted curves. The comparison shows that effect of  $C_u$  determined using sub-rounded river gravel (Menq, 2003) is less significant for crushed gravels used in this study. Also, it should be noted that model recommended by Menq (2003) is based on dry specimens with few to no fines, maximum particle size of 25 mm,  $19.1 \text{ mm} \geq D_{50} \geq 0.11 \text{ mm}$ ,  $50 \geq C_u \geq 1.1$ ,  $405 \text{ kPa} \geq \sigma'_0 \geq 14.2 \text{ kPa}$ , and  $1.1 \geq e \geq 0.23$ , and some of the tested gravel specimens are outside of this range.

## 6 CONCLUSIONS

The RCTS tests were performed on two types of compacted, crushed gravel produced in a rock quarry, with one of them being poorly-graded and the other one being relatively well-graded. The results show that for the same type of material, neither test frequency nor relative density (or void ratio) affects the  $G/G_{max} \sim \log(\gamma)$  curves significantly. The factors that most affect the  $G/G_{max} \sim \log(\gamma)$  curves are confining pressure and grain size distribution (expressed by  $C_u$ ). Similar to sandy material, the compacted gravel behaves more linearly with increasing confining pressure. Also, under the same confining pressure, the poorly-graded gravel behaves more linearly than the well-graded gravel.

Comparisons with published curves also show that the  $G/G_{max} \sim \log(\gamma)$  curves of the well-graded gravel agree well with the typical  $G/G_{max} \sim \log(\gamma)$  curves of gravelly soils suggested by Seed et al. (1986), while those of the poorly-graded gravel are within the range recommended by Rollins et al. (1998). However, the effect of confining pressure is neglected in each set of the published curves. The equation based on sub-rounded river gravel suggested by Menq (2003) to describe the  $G/G_{max} \sim \log(\gamma)$  relationship correctly indicates the effect of  $C_u$  on the  $G/G_{max} \sim \log(\gamma)$  curves, but comparison with this study shows the effect of  $C_u$  is somewhat different for crushed gravel.

## 7 REFERENCES

Darendeli B.M. 2001. *Development of a new family of normalized modulus reduction and material damping curves*. Ph. D. Dissertation, Univ. of Texas at Austin, TX, USA, 362.

Goto S., Nishio S. and Yoshimi Y. 1994. Dynamic properties of gravels sampled by ground freezing. *Ground failures under seismic conditions*. GSP No. 44, ASCE, 141-157.

Goto S., Suzuki Y., Nishio S. and Oh-oka H. 1992. Mechanical properties of undisturbed tone-river gravel obtained by in-situ freezing method. *Soils and Foundations*, 32 (3): 15-25.

Hatanaka M. and Uchida A. 1994. Effects of test methods on the cyclic deformation characteristics of high quality undisturbed gravel samples. *Static and dynamic properties of gravel soils*, GSP No. 56, ASCE, 136-151.

Hwang S.K. 1997. *Investigation of the dynamic properties of natural soils*, Ph.D. Dissertation, University of Texas at Austin, 394.

Ishihara K. 1996. *Soil behavior in earthquake geotechnics*, Oxford Science Publications, 350.

Kokusho T. 1980. Cyclic triaxial test of dynamic soil properties for wide strain range. *Soils and Foundations*, 20: 45-60.

Kokusho T. and Tanaka Y. 1994. Dynamic properties of gravel layers investigated by in-situ freezing sampling. *Ground failures under seismic conditions*. GSP No. 44, ASCE, 121-140.

Lin S.Y., Lin P.S., Luo H.S., Juag C.H. 2000. Shear modulus and damping ratio characteristics of gravelly deposits. *Canadian Geotechnical J.* 37:638-651.

Menq F.Y. 2003. *Dynamic properties of sandy and gravelly soils*, Ph.D. Dissertation, University of Texas at Austin, TX, USA, 364.

Menq F.Y. and Stokoe K.H. 2003. Linear dynamic properties of sandy and gravelly soils from large-scale resonant tests. *Deformation Characteristics of Geomaterials*, Swets & Zeitlinger, Lisse, 63-71.

Ni S.H. 1987. *Dynamic Properties of Sand Under True Triaxial Stress States from Resonant Column/Torsional Shear Tests*. Ph.D. Dissertation, University of Texas at Austin, TX, USA, 421.

Rollins K.M., Evans M., Diehl N. and Daily W. 1998. Shear modulus and damping relationships for gravels. *J. of Geotechnical and Geoenvironmental Engrg.*, 124 (5), 396-405.

Seed H.B., Wong R.T., Idriss I.M., and Tokimatsu K. 1986. Moduli and damping factors for dynamic analyses of cohesionless soils. *J. of Geotechnical Engineering*, 112 (11), 1016-1032.

Zhang J., Andrus R.D., and Juang C.H. 2005. Normalized Shear Modulus and Material Damping Relationships. *J. of Geotechnical and Geoenvironmental Engineering*, 131(4): 453-464.